# Characterization of Bending Strength in Similar and Dissimilar Carbon-Fiber-Reinforced Polymer/Aluminum Single-Lap Adhesive Joints

Jamal Bidadi [1], Hamed Saeidi Googarchin [1,*], Alireza Akhavan-Safar [2], Ricardo J. C. Carbas [2,*] and Lucas F. M. da Silva [3]

[1]  Automotive Fluid and Structures Analysis Research Laboratory, School of Automotive Engineering, Iran University of Science and Technology (IUST), Tehran 13114-16846, Iran; jamal.bidadi@gmail.com

[2]  Institute of Science and Innovation in Mechanical and Industrial Engineering (INEGI), 4200-465 Porto, Portugal; aakhavan-safar@inegi.up.pt

[3]  Department of Mechanical Engineering, Faculty of Engineering, University of Porto, 4099-002 Porto, Portugal; lucas@fe.up.pt

*  Correspondence: hsaeidi@iust.ac.ir (H.S.G.); rcarbas@fe.up.pt (R.J.C.C.)

**Abstract:** In recent years, the adhesive bonding method has gained increased attention, especially in the automotive industry, for constructing efficient body structures from dissimilar and lightweight materials such as aluminum and polymeric composites. Adhesively bonded automotive structures endure complicated loading conditions, including tensile and bending loading, during their service lives. To the best of the authors' knowledge, there is no published work on the assessment of bending strength in single-lap adhesive joints (SLJs) when considering dissimilar adherends under three-point bending. In this study, three-point bend experiments were carried on the bending strength and the failure mechanisms of dissimilar SLJs made of carbon-fiber-reinforced polymer (CFRP) and aluminum substrates bonded with Araldite 2015 adhesive. Additional experiments were conducted individually on similar SLJs, including aluminum/aluminum and CFRP/CFRP, to investigate and compare the effects of adherend material type on the bending strength and failure behavior of SLJs. The results indicate that a CFRP/CFRP single-lap adhesive joint exhibits significantly higher joint strength in comparison to an aluminum/aluminum single-lap adhesive joint under three-point bending. The strength of dissimilar CFRP/aluminum single-lap joints usually falls between that of an aluminum/aluminum and that of a CFRP/CFRP single-lap adhesive joint. When the CFRP adherend is situated at the bottom of the joint in three-point bending, it imparts significantly greater joint strength and deformation compared to situations where the aluminum adherend is placed at the bottom.

**Keywords:** adhesive; CFRP/aluminum hybrid joint; bending strength; single-lap joint

## 1. Introduction

One of the critical issues in automotive engineering is the reduction of fuel consumption. In this context, reducing the car's weight is considered an effective solution. Polymer composites and aluminum sheets are strongly preferred in the automotive industry due to their lighter weight compared to steel. In recent years, there has been a growing trend of the use of adhesives for connecting load-bearing components [1–4]. Within the automotive industry, designers seek to create lighter and more cost-effective vehicles by incorporating a diverse range of dissimilar materials [5,6]. The primary challenge when working with these dissimilar materials is the identification of a suitable joining method. For example, spot welding stands out as the most commonly employed joining technique in the automotive sector [7,8]. However, spot welding comes with certain disadvantages, such as the requirement for access to both sides of the parts to be welded, limitations on welding

between aluminum and composite materials, and potential damage to coated surfaces due to high heat exposure. In contrast, adhesive bonding technology offers a compelling solution to these challenges, providing a wide array of advantages [9]. These advantages include ensuring uniform stress distribution within the bonding area, enhancing fatigue and impact resistance, reducing stress concentration in the bonded region, and facilitating the joining of dissimilar materials. Adhesives can offer versatile applications throughout the car bodyshell, with these applications being influenced by factors such as adhesive stiffness, strength, and the specific placement of the adhesive within the bodyshell. For instance, certain nonstructural adhesives with lower strength (like polyurethanes [10,11]) are employed for purposes such as sealing or creating joints in regions of the vehicle that are not considered structural components. Conversely, other types of structural adhesives with greater strength, such as epoxy-based adhesives [9,12], find use in creating joints between structural elements such as chassis parts or metallic and non-metallic thin-walled critical components of a car's bodyshell. Consequently, the uses of adhesives can be neatly categorized into two distinct groups: structural (a connection that must bear significant forces) and nonstructural adhesive joints. In recent years, polymeric composite materials have emerged as crucial components within the automotive industry, bringing about a transformation in vehicle design, manufacturing, and performance. These sophisticated materials, typically comprising a polymer matrix reinforced with fibers or particles, offer a wide array of advantages and have applications in the automotive sector. Their benefits include weight reduction, enhanced fuel efficiency, bolstered structural integrity, and noise, vibration, and harshness (NVH) reduction. The integration of polymeric composites with traditional metals in car bodyshell manufacturing can be accomplished through a variety of methods. These methods include mechanical fasteners, adhesive bonding, bolt and nut, and clinching, each possessing distinct advantages and disadvantages. The selection of a particular joining method hinges upon factors such as the specific materials in use, structural requirements, manufacturing processes, and constraints. Most recently, there has been an increasing trend in the utilization of adhesively bonded hybrid components comprising polymeric fiber-reinforced composites and other lightweight metallic materials, such as aluminum alloys, across various sectors, including automotive and civil engineering.

To enhance our understanding of the application of structural adhesive joints in the automotive and other sectors, it is imperative to characterize the mechanical and fracture behavior of joints between various types of polymeric and metallic materials. In recent years, single-lap joint geometry has gained recognition as a well-established test configuration for assessing adhesive bond strength in joints. This type of adhesive joint may be subjected to various types of loading, including tension, bending, and combinations of both tension and bending conditions. Until now, extensive analytical [13–15], experimental [16,17], and numerical [18], refs. [19–22] research efforts have been dedicated to single-lap adhesive joints subjected to tension. For example, some primary analytical solutions were proposed by Goland and Reissner [23] and Volkerson [24], and other researchers [14,25,26] for evaluating the stress distribution within single-lap adhesive joints under tension, including considering parameters such as adherend bending effect, adhesive and adherend plasticity, stress at free edges, composite adherend, and adhesive spew fillets. Subsequently, numerical approaches based on finite element methods have been introduced to simulate and assess the stress distribution in complex adhesive joints, such as single-lap joints, which consider material and geometrical nonlinearities in the analysis.

Automotive components need to maintain their integrity over the vehicle's lifespan. In comparison to tension loading, the behavior of single-lap adhesive joints under bending loading has not received extensive investigation. However, it is worth noting that, in real applications, adhesive joints can experience a variety of conditions, including three-point and four-point loading conditions. Understanding the bending strength of adhesive joints ensures safety and reliability, reducing the risk of structural failure while the vehicle is in use. For example, in braking and accelerating conditions of an automobile, a bending load can be imposed on adhesive joints. Therefore, studying the bending behavior of adhesive

joints helps simulate real-world scenarios where bending forces may be prevalent, ensuring that the joints can endure these conditions without failure [27,28]. Only a few papers that analyze the bending behavior of single-lap adhesive joints can be found. For example, Liu et al. [29] investigated the four-point bending behavior of single-lap adhesive joints both experimentally and theoretically. Ozel et al. [30] conducted a study on the four-point bending behavior of single-lap joints with high-strength steel adherends, investigating the impact of adherend thickness, adherend overlap, and adhesive type. Aydin et al. [31] conducted a series of experimental and numerical analyses on single-lap adhesive joints consisting of AA2024-T3 adherends with three different overlap lengths and two types of adhesives. Their research revealed that the bending strength of these single-lap adhesive joints increases as the overlap length increases. Furthermore, they demonstrated that a failure in a single-lap joint initiates from the overlap region at the interface between the adhesive and the upper adherend in tension and then propagates toward the center of the overlap. Akpinar and Aydin [32] conducted a three-dimensional numerical stress analysis on single-lap adhesive joints composed of composite adherends subjected to four-point bending loading. In their study, they examined the influence of the fiber orientation angle of laminate composites on stress distributions and the prediction of failure in single-lap adhesive joints. Their findings demonstrated that the ply stacking sequence has a substantial impact on both stress distribution and the failure behavior of single-lap adhesive joints under four-point bending loads. A few papers can also be found on the subject of three-point bending loading conditions of single-lap adhesive joints. For instance, Kadioglu and Demiral [33] investigated the three-point bending behavior of single-lap adhesive joints composed of angle-plied glass-reinforced polymer-matrix laminate composite adherends with three different stacking sequences. They also studied the effects of the overlap length, adherend thickness, and the thickness of the adhesive layer on the damage mechanisms in the adhesive layer and composite adherends. In another study, Demiral and Kadioglu [34] investigated the three-point bending behavior of step lap adhesive joints composed of AA2024-T3 adherends. They stated that a joint with three steps has the best flexural performance, and the amount of energy absorption increases with increasing overlap length at the upper and lower steps.

A review of the literature indicates that no study has yet been conducted on the three-point bending behavior of dissimilar composite/aluminum single-lap adhesive joints. Therefore, the aim of this study was to investigate the strength of single-lap composite/aluminum adhesive joints under three-point bending loading. The behavior of joints was also experimentally examined when similar aluminum/aluminum and composite/composite adherends were used.

## 2. Experimental Procedure

### 2.1. Materials

#### 2.1.1. Adhesive

Araldite 2015 was used as the adhesive material. This two-component epoxy adhesive is commonly used in various industries for structural bonding applications and is suitable for bonding a wide range of materials, including metals, ceramics, glass, rubber, and most plastics in the aerospace, automotive, and construction industries. Table 1 represents the mechanical and fracture properties of Araldite 2015.

#### 2.1.2. Adherends

- Metallic adherend

The aluminum alloy (AA6061-T6) was used as the metallic adherend material. This type of aluminum alloy is widely used in the manufacture of new car bodyshells. Test samples were cut from a rolled plate. Table 2 presents the mechanical properties of the aluminum alloy.

- Composite adherend

Carbon-fiber-reinforced polymer (CFRP) composite laminates were employed as the composite adherend in this study, showcasing their significance in modern engineering applications. These CFRP adherends were cut from a unidirectional composite plate. The primary composite plate was fabricated using the hand layup process, as depicted in the schematic presented in Figure 1. The hand layup process involved the sequential layering of 12 unidirectional carbon-fiber sheets and the application of LY-5052 epoxy resin, each accounting for 50% of the total composite mass. This process yields a composite plate distinguished by its controlled fiber orientation and customized material properties. The mechanical properties of the fabricated carbon-fiber sheets were determined via standard tests. As per the guidelines outlined in ASTM D3039/D3039M [35], the composite's tensile properties can be evaluated in multiple directions, both along the fiber orientation (referred to as the 1-axis in Figure 1e) and perpendicular to the fiber direction (referred to as the 2-axis in Figure 1e). These tests are conducted under quasi-static conditions, offering a comprehensive understanding of the composite's mechanical behavior in different orientations. Furthermore, to determine the composite's shear properties, ASTM D3518/D3518M [36] provides a reliable framework and methodology. The schematics of the performed tests are displayed in Figure 2. Table 3 represents the measured mechanical properties of the fabricated CFRP plate.
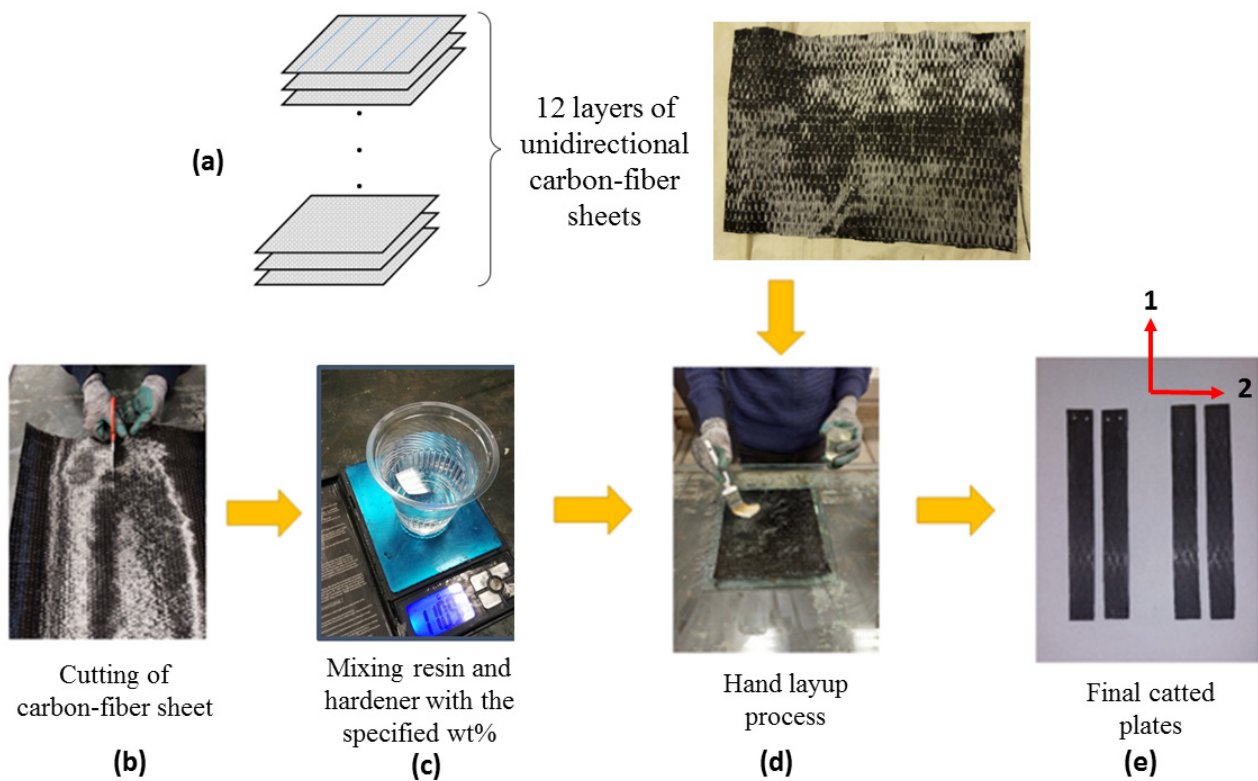


**Figure 1.** The hand layup process for fabrication of CFRP laminate, (**a**) Schematic of the hand layup process, (**b**) Cutting process of carbon fiber sheet, (**c**) Mixing the resin and hardener, (**d**) Hand layup step, (**e**) Fabricated samples (Indices 1 and 2 shown in figure (**e**) indicate the parallel and perpendicular directions of the fibers, respectively).

(**a**) Tensile test along the
fiber orientation

(**b**) Tensile test perpendicular
to the fiber direction
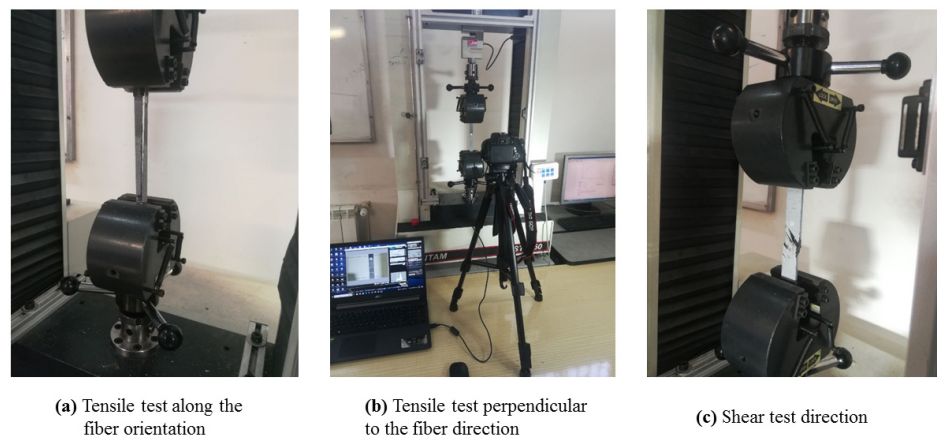
(**c**) Shear test direction

**Figure 2.** The quasi-static tests conducted to determine the mechanical properties of the CFRP, (**a**) Tensile test parallel in the directions of the fibers, (**b**) The camera setup, (**c**) Tensile test in the perpendicular directions of the fibers.

**Table 1.** The mechanical and fracture properties of Araldite 2015 [37].

| Property | Value |
|---|---|
| Young's modulus, $E$ (MPa) | 1850 |
| Poisson's ratio, $\nu$ | 0.33 |
| Tensile yield strength, $\sigma_y$ (MPa) | 12.63 |
| Tensile strength, $\sigma_f$ (MPa) | 21.63 |
| Tensile failure strain, $\varepsilon_f$ (%) | 4.77 |
| Shear modulus, $G$ (MPa) | 700 |
| Shear yield strength, $\tau_y$ (MPa) | 14.6 |
| Shear strength, $\tau_f$ (MPa) | 17.9 |
| Shear failure strain, $\gamma_f$ (%) | 43.9 |
| Fracture toughness in tension, $G_{IC}$ (N/mm) | 0.43 |
| Fracture toughness in shear, $G_{IIC}$ (N/mm) | 4.77 |

**Table 2.** The mechanical properties of 6061-T6 aluminum alloy [9].

| Property | Value |
|---|---|
| Young's modulus, $E$ (GPa) | 68.9 |
| Poisson's ratio, $\nu$ | 0.33 |
| Tensile yield strength, $\sigma_y$ (MPa) | 276 |
| Tensile ultimate strength, $\sigma_u$ (MPa) | 310 |
| Rapture strain, $\varepsilon_f$ (%) | 17 |

**Table 3.** The mechanical and fracture properties of CFRP plate.

| Property | Value |
|---|---|
| Fiber direction Young's modulus, $E_{11}$ (GPa) | 109 |
| Perpendicular to the fiber direction Young's modulus, $E_{22}$ (GPa) | 92 |
| Poisson's ratio, $\nu_{21}$ | 0.037 |
| Shear modulus, $G_{12}$ (GPa) | 8.5 |
| Shear modulus, $G_{13}$ (GPa) | 7.3 |

### 2.2. Specimen Geometry

The geometry of the single-lap joint is illustrated in Figure 3. In this context, the single-lap test was employed to assess the bending strengths of the adhesives under three-point bending loading conditions. The overlap length, adhesive thickness, and adherend thickness were selected as 30 mm, and 0.4 mm, and 4 mm, respectively.
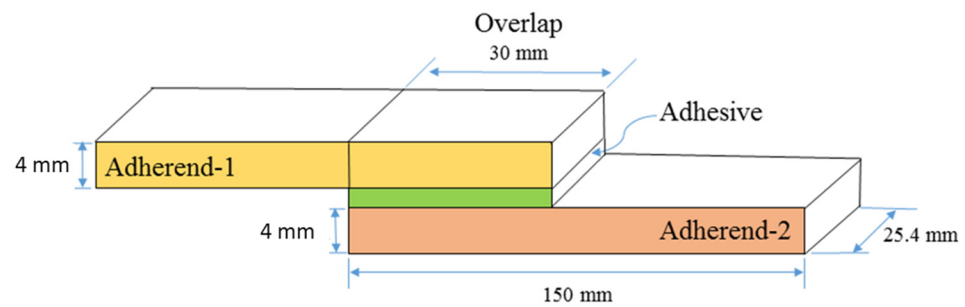
**Figure 3.** Single-lap adhesive joint geometry (not to scale).

### 2.3. Specimen Fabrication

Surface preparation for the aluminum adherend was carried out through a two-step process. Initially, the aluminum adherend underwent polishing using 200-grit sandpaper at an angle of ±45 degrees. Subsequently, a thorough cleaning of the bonding surfaces was conducted using 100% industrial acetone and a sterile bandage. This cleaning procedure involved multiple steps to thoroughly remove any residual fine particles resulting from the sanding process and potential dust particles from the laboratory environment. As for the CFRP adherents, their surface preparation involved polishing using 800-grit sandpaper at an angle of ±45 degrees, followed by cleaning with 100% industrial acetone. Moving forward, the adhesive was applied to the bonding surfaces per the manufacturer's datasheet, adhering at the recommended resin-to-hardener ratio of 1:1 by weight. Special fixtures were utilized to securely hold together the adhesive-impregnated surfaces, ensuring precise alignment. Additionally, the thickness of the adhesive layer was meticulously controlled by inserting metallic shims. All specimens then underwent a curing process at room temperature, which lasted one week. The final bonded joints are shown in Figure 4. This detailed preparation and curing regimen was critical to ensure the consistency and reliability of the test results.
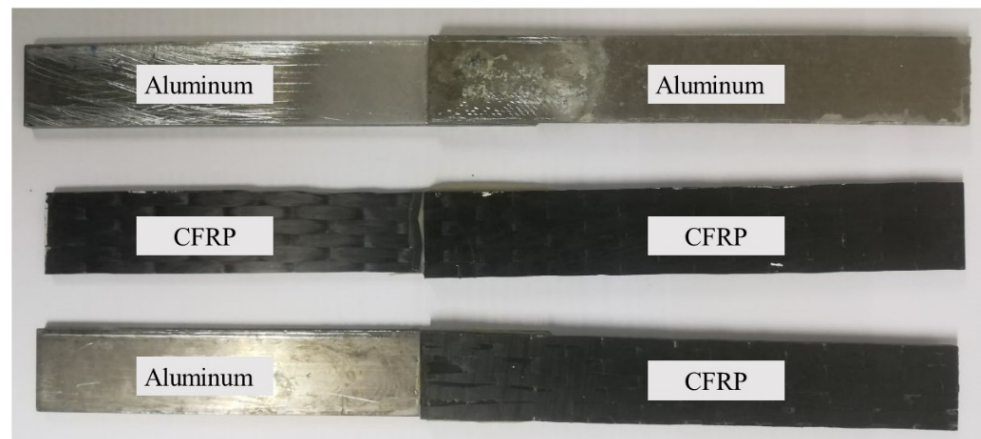


**Figure 4.** The fabricated single-lap adhesive joints.

### 2.4. Test Procedure

The loading condition depicted in Figure 5 was employed for the three-point bending tests of single-lap adhesive joints. The distance between the inner loading point (located at the center of the overlap) and the outer supports (denoted as "S" in Figure 5) was set at 120 mm. Here, the goal was to use the maximum sample length to create a larger moment at the bonded area. In preparation for the bending test, a small metallic/polymeric patch was attached to the end of the joint, as depicted in Figure 5. As depicted in the schematic representation in Figure 6, the samples underwent a quasi-static three-point bending test under displacement control conditions at a rate of 1 mm/min. It should be noted that,

each test was replicated three times. This testing was conducted using a pneumatic testing machine manufactured by SANTAM in Iran. The load–displacement curves were measured using a 2.5-ton load cell.
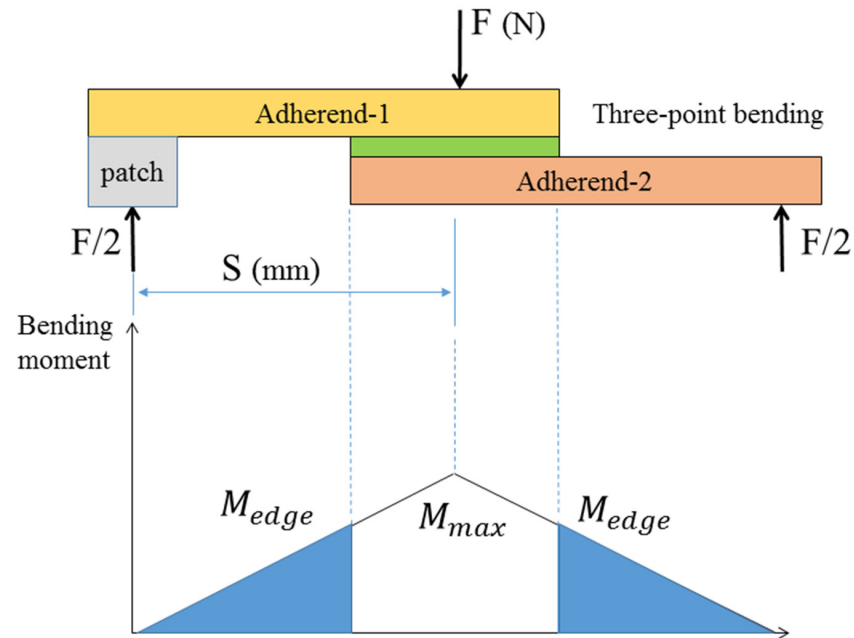


**Figure 5.** The three-point bending test and the respective bending moment diagram. The blue regions represent the moment outside the overlap length.
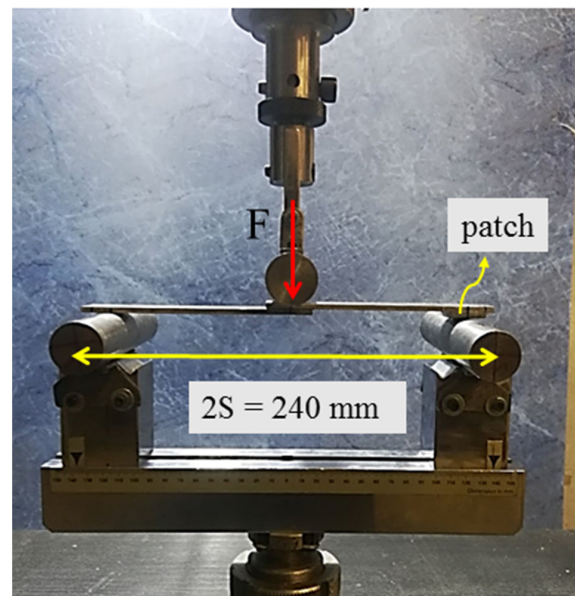


**Figure 6.** The three-point test of single-lap adhesive joint (Al-Al).

### 3. Results and Discussion

As previously mentioned, all samples maintained a constant overlap length of 30 mm, joint width of 25 mm, and a distance between loading points (S) equal to 120 mm. The only variation lay in the type of adherent materials used. Specifically, the single-lap adhesive joints were constructed using combinations of aluminum/aluminum, CFRP/CFRP, and CFRP/aluminum materials. The typical load–displacement plots for the tested single-lap adhesive joints under three-point bending loading conditions are depicted in Figure 7. These experimental results and pictures of the fractured surfaces are shown in Table 4

and Figure 8, respectively. As can be seen from Figure 8, the fracture surface patterns are combinations of cohesive (a type of failure so that a layer of adhesive remains on both surfaces of the adherends) and adhesive (interfacial bond failure between the adhesive layer and the surfaces of the substrate) failures. These types of failures of the single-lap adhesive joints are also reported in many papers authored by different researchers [2,10,11].
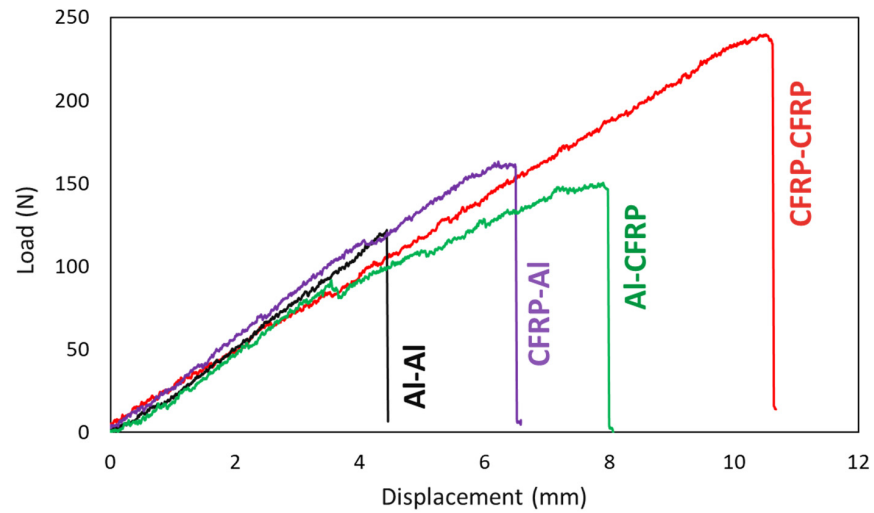


**Figure 7.** The typical load–displacement curves for the tested single-lap adhesive joints under three-point bending loading conditions.

**Table 4.** Experimental results of single-lap adhesive joints under three-point bending loading.

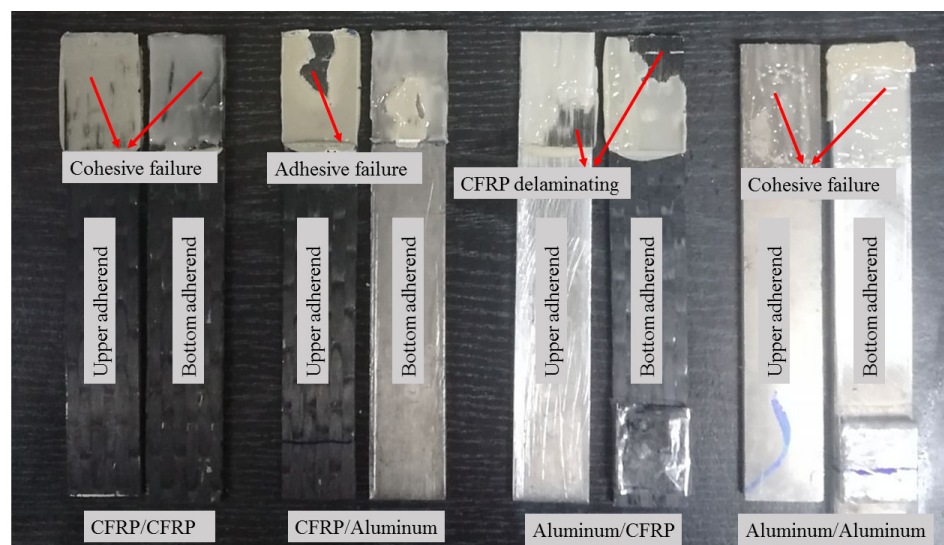| Top/Bottom Adherend Materials | Average Peak Load (N) | Maximum Bending Moment at the Edge of the Overlap (N m) | Displacement at Peak Load (mm) |
|---|---|---|---|
| Aluminum/Aluminum | $125.1 \pm 7.9$ | 7.5 | $4.5 \pm 0.3$ |
| CFRP/CFRP | $242.8 \pm 18.2$ | 14.5 | $12 \pm 1.3$ |
| CFRP/Aluminum | $147.2 \pm 17.7$ | 8.8 | $5.2 \pm 0.9$ |
| Aluminum/CFRP | $154.5 \pm 19.1$ | 9.25 | $8 \pm 1.5$ |



**Figure 8.** The fractured surface of the tested single-lap adhesive joints under three-point bending loading conditions.

The deformed shape of the single-lap adhesive joint under three-point bending is depicted in Figure 9, which was described according to the principles of beam mechanics theory in bending loading conditions. In this illustration, it becomes evident that the bottom region of the neutral axis experiences tensile stress, while the upper regions, located above the neutral axis, undergo compression stress. As a result, any failure would originate from the side experiencing tensile stress, specifically the lower part of the neutral axis. Conversely, no failures occurred in the adhesive above the neutral axis. Figure 10 further confirms this phenomenon, as observed in the tested single-lap joint specimens. In this figure, it is evident that crack initiation and propagation have occurred from the lower section of the joint, precisely at the interface between the adhesive layer and the lower adherend (here, the aluminum plate), where tensile stresses dominate. In other words, the crack near the interface is expanding, and it might experience kinking as it progresses toward the upper interface. However, the failure is cohesive in nature because a thin layer persists on the lower adhesive surface (Figure 8). As shown in Table 4, notably, there is a clear correlation between the displacement at peak loads and the joint's strength. Specifically, the CFRP/CFRP configuration showed the highest displacement, surpassing that of the aluminum/aluminum single-lap adhesive joints by 167%. This behavior can be attributed to the varying stiffnesses of the aluminum and CFRP adherends. Notably, the CFRP adherend offers greater flexibility compared to the aluminum adherend, as indicated by their respective Young's modulus values, as shown in Tables 2 and 3.
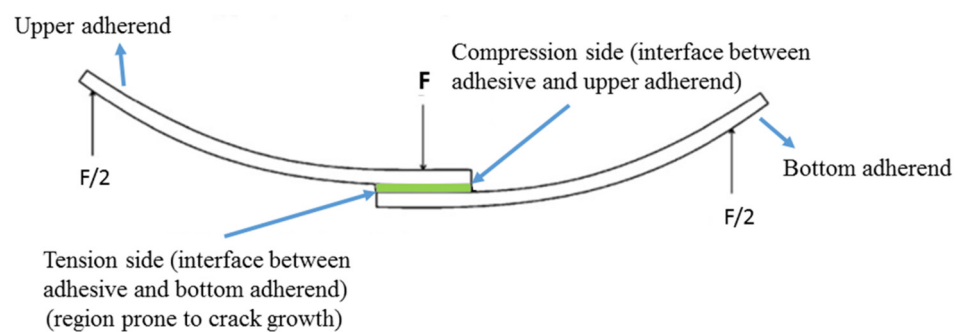


**Figure 9.** The deformation of the single-lap adhesive joints under three-point bending loading conditions.
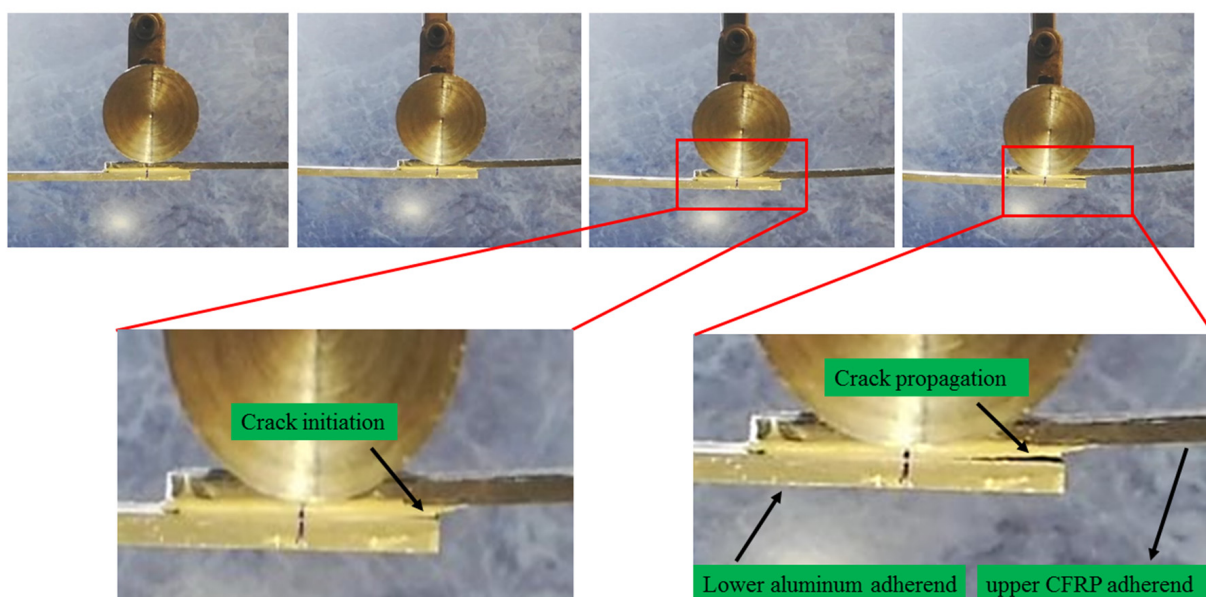


**Figure 10.** The crack initiation and propagation of the single-lap adhesive joints from the interface between the upper adherend (here the CFRP plate) and the lower adherend (here the aluminum plate).

As previously illustrated in Figure 5, the bending moment in the three-point bending test follows a linear variation. Its highest point is achieved at the midpoint of the overlap and subsequently diminishes in a linear manner until it reaches a value of zero at the outer supports. Consequently, the moment at the edges ($M_{edge}$) of the single-lap adhesive joint can be expressed in terms of the maximum moment ($M_{max}$), the distance between the applied load (F) location and the outer support (S), and the overlap length (OL), as follows [38]:

$$M_{edge} = M_{max}(1 - \frac{OL}{2S}) \quad \text{where} \quad M_{max} = \frac{F \times S}{2} \tag{1}$$

The bending moments at the edges of the overlap are provided in Table 4 by inserting the experimental failure load into Equation (1). This reveals that the bending moments at the edges of the overlap are directly proportional to the peak loads sustained by the joints (Figure 11). Consequently, the CFRP/CFRP single-lap adhesive joints experience the highest bending moments before failure, while the aluminum/aluminum single-lap adhesive joints exhibit the lowest bending strength at the edge points. In simpler terms, the bending moment at the edge of the overlap is dictated by the load carried by the joint as well as the types of adherends, which encompasses various adherend combinations, such as CFRP/CFRP, aluminum/aluminum, and two scenarios involving CFRP/aluminum and aluminum/CFRP. Hence, it can be concluded that a larger bending moment at the edges of the overlap results in a greater force at the midpoint of the overlap length. It should be noted that some other factors, such as environmental conditions and loading rate, can be investigated as a subject of future research.
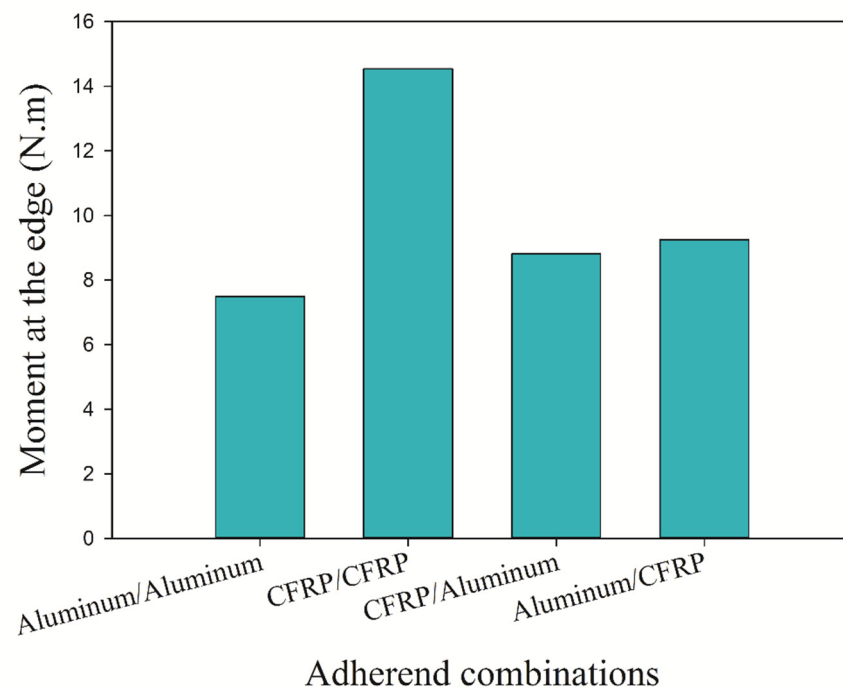


**Figure 11.** Bending moment at the edge of the overlap at the point of failure for the different adherend combinations in the single-lap adhesive joints during three-point bending.

## 4. Conclusions

The behavior of single-lap adhesive joints used in the automotive and aerospace industry was investigated under three-point bending loading conditions. Various combinations of adherend such as aluminum/aluminum, CFRP/CFRP, and aluminum/CFRP were studied. The parameters of overlap length, adhesive thickness, and the distance between loading points were constants during the bending tests. The main conclusions are as follows:

(1) The strength of single-lap joints under three-point bending was related to the type of adherend materials, so that the materials with lower stiffness (polymeric composites) provide better joint strength compared with materials of greater stiffness (metallic materials).

(2) A CFRP/CFRP single-lap adhesive joint exhibits significantly higher joint strength in comparison to an aluminum/aluminum single-lap adhesive joint under three-point bending. This distinction highlights the superior performance and load-bearing capacity of the CFRP/CFRP joint configuration, making it an advantageous choice for applications requiring robust structural integrity and durability.

(3) In the context of a single-lap adhesive joint under three-point bending, it is important to note that the regions located below the neutral axis are subjected to tensile stress. Conversely, the areas situated above the neutral axis experience compressive stress. This stress distribution is a critical consideration in the analysis of joint behavior under three-point bending loading conditions, as it directly influences the structural response and integrity of the adhesive bond.

(4) The strength of dissimilar CFRP/aluminum single-lap joints is usually linked to the placement of the adherends, whether they are positioned at the top or bottom of the joint structure. Notably, when the CFRP adherend is situated at the bottom, it imparts significantly greater joint strength and deformation compared to situations where the aluminum adherend is placed at the bottom. This observation underscores the critical role that adherend positioning plays in determining the overall load-bearing capacity and performance of these joints under three-point bending.

(5) In addition to its superior bending strength, the CFRP/CFRP joint configuration also displayed the largest displacement at failure, surpassing the aluminum/aluminum single-lap adhesive joints by 167%.

## References

1. Shishesaz, M.; Ghamarian, A.H.; Moradi, S. Stress distribution in laminated composite tubular joints with damaged adhesive layer under torsion. *J. Adhes.* **2023**, *99*, 930–971. [CrossRef]

2. Liu, J.; Guo, T.; Hebdon, M.H.; Liu, Z.; Wang, L. Bonding Behaviors of GFRP/Steel Bonded Joints after Wet–Dry Cyclic and Hygrothermal Curing. *Appl. Sci.* **2020**, *10*, 5411. [CrossRef]

3. Barile, C.; Casavola, C.; Moramarco, V.; Pappalettere, C.; Vimalathithan, P.K. Bonding Characteristics of Single- and Joggled-Lap CFRP Specimens: Mechanical and Acoustic Investigations. *Appl. Sci.* **2020**, *10*, 1782. [CrossRef]

4. Tan, W.; Na, J.X.; Zhou, Z.F. Effect of temperature and humidity on the creep and aging behavior of adhesive joints under static loads. *J. Adhes.* **2023**, *99*, 672–690. [CrossRef]

5. Marannano, G.; Zuccarello, B. Numerical experimental analysis of hybrid double lap aluminum-CFRP joints. *Compos. Part B Eng.* **2015**, *71*, 28–39. [CrossRef]

6. Maggiore, S.; Banea, M.D.; Stagnaro, P.; Luciano, G. A review of structural adhesive joints in hybrid joining processes. *Polymers* **2021**, *13*, 3961. [CrossRef]

7. Ambroziak, A.; Korzeniowski, M. Using resistance spot welding for joining aluminium elements in automotive industry. *Arch. Civ. Mech. Eng.* **2010**, *10*, 5–13. [CrossRef]

8. Pouranvari, M.; Marashi, S.P.H. Critical review of automotive steels spot welding: Process, structure and properties. *Sci. Technol. Weld. Join.* **2013**, *18*, 361–403. [CrossRef]

9.    Bidadi, J.; Miandowab, H.H.; Googarchin, H.S. Experimental and Numerical Investigation of the Performance of Automotive Adhesively Bonded Crash Box Beams Under Transverse Loading. *Automot. Sci. Eng.* **2023**, *13*, 4085–4091.

10.   Obayashi, K.; Kamitani, K.; Chu, C.-W.; Kawatoko, R.; Cheng, C.-H.; Takahara, A.; Kojio, K. Deformation Behavior of Polyurethane Adhesive in the Single-Lap Joint Based on the Microbeam X-ray Scattering Method. *ACS Appl. Polym. Mater.* **2022**, *4*, 5387–5394. [CrossRef]

11.   Chen, H.; Wang, D.; Na, J.; Chen, X.; Meng, H. Strength evaluation of polyurethane elastomeric bonded joints under extreme service conditions. *Int. J. Adhes. Adhes.* **2023**, *123*, 103344. [CrossRef]

12.   Bidadi, J.; Googarchin, H.S.; Akhavan-Safar, A.; da Silva, L.F.M. Loading rate effects on mixed-mode I/II fracture envelope of epoxy resins with nonlinear behavior. *Theor. Appl. Fract. Mech.* **2023**, *125*, 103858. [CrossRef]

13.   da Silva, L.F.M.; Neves, P.J.C.D.; Adams, R.D.; Spelt, J.K. Analytical models of adhesively bonded joints-Part I: Literature survey. *Int. J. Adhes. Adhes.* **2009**, *29*, 319–330. [CrossRef]

14.   Wang, R.X.; Cui, J.; Sinclair, A.N.; Spelt, J.K. Strength of adhesive joints with adherend yielding: I. Analytical model. *J. Adhes.* **2003**, *79*, 23–48. [CrossRef]

15.   Stein, N.; Felger, J.; Becker, W. Analytical models for functionally graded adhesive single lap joints: A comparative study. *Int. J. Adhes. Adhes.* **2017**, *76*, 70–82. [CrossRef]

16.   Zhang, K.; Li, L.; Duan, Y.; Li, Y. Experimental and theoretical stress analysis for an interface stress model of single-L adhesive joints between CFRP and aluminum components. *Int. J. Adhes. Adhes.* **2014**, *50*, 37–44. [CrossRef]

17.   Ruiz, P.D.; Jumbo, F.; Huntley, J.M.; Ashcroft, I.A.; Swallowe, G.M. Experimental and Numerical Investigation of Strain Distributions within the Adhesive Layer in Bonded Joints. *Strain* **2011**, *47*, 88–104. [CrossRef]

18.   Peres, L.M.C.; Arnaud, M.F.T.D.; Silva, A.F.M.V.; Icon, R.D.S.G.C.; Machado, J.J.M.; Marques, E.A.S.; Da Silva, L.F.M. Geometry and adhesive optimization of single-lap adhesive joints under impact. *J. Adhes.* **2022**, *98*, 677–703. [CrossRef]

19.   Lou, S.; Cheng, B.; Ren, G.; Li, Y.; Bai, X.; Chen, P. Effect of adhesive modification and surface treatment of laminates on the single lap bonding joint properties of carbon fibre composites. *J. Adhes.* **2023**, *99*, 1916–1932. [CrossRef]

20.   Ma, G.; Han, X.; Ying, L.; Wang, D.; Wu, C. Mechanical performance of adhesively bonded carbon fiber reinforced boron-modified phenolic resin plastic-titanium single-lap joints at high temperature. *Polym. Compos.* **2023**. [CrossRef]

21.   Chen, Q.; Du, B.; Zhang, X.; Zhong, H.; Ning, C.; Bai, H.; Li, Q.; Pan, R.; Zhou, B.; Hu, H. Parametric Investigation into the Shear Strength of Adhesively Bonded Single-Lap Joints. *Materials* **2022**, *15*, 8013. [CrossRef]

22.   Papanicolaou, G.C.; Kontaxis, L.C.; Portan, D.V.; Petropoulos, G.N.; Valeriou, E.; Alexandropoulos, D. Mechanical Performance Enhancement of Aluminum Single-Lap Adhesive Joints Due to Organized Alumina Nanotubes Layer Formation on the Aluminum Adherends. *Appl. Nano* **2021**, *2*, 206–221. [CrossRef]

23.   Goland, M.; Reissner, E. The Stresses in Cemented Joints. *J. Appl. Mech. Trans. ASME* **1944**, *11*, A17–A27. [CrossRef]

24.   Volkersen, O. Die Nietkraftverteilung in zugbeanspruchten Nietverbindungen mit konstanten Laschenquerschnitten. *Luftfahrt-forschung* **1938**, *15*, 41–47. Available online: https://cir.nii.ac.jp/crid/1570009751444198272 (accessed on 12 October 2023).

25.   Crocombe, A.D.; Bigwood, D.A. Development of a full elasto-plastic adhesive joint design analysis. *J. Strain Anal. Eng. Des.* **1992**, *27*, 211–218. [CrossRef]

26.   Mortensen, F.; Thomsen, O.T. Analysis of adhesive bonded joints: A unified approach. *Compos. Sci. Technol.* **2002**, *62*, 1011–1031. [CrossRef]

27.   Wu, W.; Liu, Q.; Zong, Z.; Sun, G.; Li, Q. Experimental investigation into transverse crashworthiness of CFRP adhesively bonded joints in vehicle structure. *Compos. Struct.* **2013**, *106*, 581–589. [CrossRef]

28.   Silva, M.R.G.; Marques, E.A.S.; da Silva, L.F.M. Behaviour under Impact of Mixed Adhesive Joints for the Automotive Industry. *Lat. Am. J. Solids Struct.* **2016**, *13*, 835–853. [CrossRef]

29.   Liu, J.; Sawa, T.; Toratani, H. A two-dimensional stress analysis and strength of single-lap adhesive joints of dissimilar adherends subjected to external bending moments. *J. Adhes.* **1999**, *69*, 263–291. [CrossRef]

30.   Özel, A.; Aydin, M.D.; Temiz, Ş. The effects of overlap length and adherend thickness on the strength of adhesively bonded joints subjected to bending moment. *J. Adhes. Sci. Technol.* **2004**, *18*, 313–325. [CrossRef]

31.   Aydin, M.D.; Özel, A.; Temiz, Ş. Non-linear stress and failure analyses of adhesively-bonded joints subjected to a bending moment. *J. Adhes. Sci. Technol.* **2004**, *18*, 1589–1602. [CrossRef]

32.   Akpinar, S.; Aydin, M.D. 3-D non-linear stress analysis on the adhesively bonded composite joint under bending moment. *Int. J. Mech. Sci.* **2014**, *81*, 149–157. [CrossRef]

33.   Kadioglu, F.; Demiral, M. Failure behaviour of the single lap joints of angle-plied composites under three point bending tests. *J. Adhes. Sci. Technol.* **2020**, *34*, 531–548. [CrossRef]

34.   Demiral, M.; Kadioglu, F. Damage Characteristics of a Step Lap Joint Exposed to Flexural Loading for Its Different Configurations. *Polymers* **2023**, *15*, 2458. [CrossRef]

35.   *D3039/D3039M*; Standard Test Method for Tensile Properties of Polymer Matrix Composite Materials. Annual Book of ASTM Standards. ASTM International: West Conshohocken, PA, USA, 2017. Available online: http://scholar.google.com/scholar?hl=en&amp;btnG=Search&amp;q=intitle:Standard+Test+Method+for+Tensile+Properties+of+Polymer+Matrix+Composite+Materials#1 (accessed on 20 October 2023).

36. *D3518*; Standard Test Method for In-Plane Shear Response of Polymer Matrix Composite Materials by Tensile Test of a 645° Laminate 1. Annual Book of ASTM Standards. ASTM International: West Conshohocken, PA, USA, 2007. Available online: https://www.astm.org/d3518_d3518m-13.html (accessed on 20 October 2023).

37. Öz, Ö.; Özer, H. An experimental investigation on the failure loads of the mono and bi-adhesive joints. *J. Adhes. Sci. Technol.* **2017**, *31*, 2251–2270. [CrossRef]

38. Grant, L.D.R.; Adams, R.D.; da Silva, L.F.M. Effect of the temperature on the strength of adhesively bonded single lap and T joints for the automotive industry. *Int. J. Adhes. Adhes.* **2009**, *29*, 535–542. [CrossRef]